

Evaluation of the performances of a novel Punch Through Trench IGBT using a $\text{Si}_{(1-x)}\text{Ge}_x \text{N}^+$ buffer layer by using finite elements simulations

S. Azzopardi, Y. Belmehdi, F. Capy, J.-Y. Deletage, E. Woirgard

IMS Laboratory – University of Bordeaux, 351 cours de la Libération, 33405 Talence Cedex, France

Abstract – In this paper, a new Punch Through Trench IGBT using a $\text{Si}_{(1-x)}\text{Ge}_x \text{N}^+$ buffer layer is investigated by using two dimensional finite elements numerical simulations. The performances of this device are mainly obtained from the reduction of the turn-off switching time for a slight elevation of the on-state voltage. A study of the main static characteristics has been performed, particularly the relevance of the trade-off between the turn-off time and the on-state voltage, and its temperature dependency. At least, a comparison with a Carrier Storage Trench-gate Bipolar Transistor and a Trench Field Stop IGBT also including a $\text{Si}_{(1-x)}\text{Ge}_x \text{N}^+$ buffer layer is done by the mean of trade off curves.

Index Terms – Power semiconductor, punch-through IGBT, hetero-junction, finite element simulations.

I. INTRODUCTION

In power electronics applications, the Insulated Gate Bipolar Transistor (IGBT) is one of the most used components, particularly for the medium power applications. The choice of the IGBT is related to the characteristics provided in terms of robustness, switching losses and on-state losses. However, the trade-off between those three characteristics has to be considered when it is useful to compare different devices.

This study consists in establishing the performances of a novel IGBT using a $\text{Si}_{(1-x)}\text{Ge}_x \text{N}^+$ buffer layer, with x representing the mole fraction of germanium in this layer. The main interest of using a $\text{Si}_{(1-x)}\text{Ge}_x$ layer is to reduce the band gap comparing to silicon layer [1-5]. A complete preliminary study has to be performed to evaluate the impact of the use of a $\text{Si}_{(1-x)}\text{Ge}_x$ layer on the trade-off performances between the on-state voltage and the turn-off time. In order to point out the main benefits of using the $\text{Si}_{(1-x)}\text{Ge}_x \text{N}^+$ buffer, it is necessary to compare the main figure of merit of the Punch Through Trench Gate IGBT without ($x=0$) and with a germanium profile in the N^+ buffer layer. This work has been performed with a help of a physically-based device simulation TCAD SENTAURUS software [7].

II. Si/SiGe JUNCTION

The originality of the proposed device is located in the use of a $\text{Si}_{(1-x)}\text{Ge}_x \text{N}^+$ buffer layer. In order to understand

the interest of using this heterostructure instead of simple silicon N^+ buffer layer, it is necessary to study the P^+ / N^+ junction. It is a $\text{Si} / \text{Si}_{(1-x)}\text{Ge}_x$ junction with x representing the mole fraction, with a profile depicted in figure 1. It means that the P region which represents the substrate is only composed of silicon ($x=0$), whereas the N^+ region representing the buffer layer is assimilated to an heterostructure $\text{Si}_{(1-x)}\text{Ge}_x$ with an abrupt profile of germanium ($x>0$). A voltage V is applied on the junction to represent the forward bias applied during the on-state of the Trench IGBT.

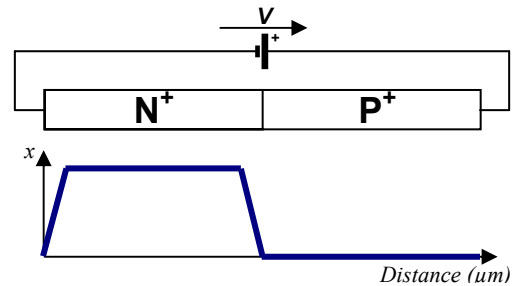


Fig.1 - The structure of the forward biased $\text{Si}_{(1-x)}\text{Ge}_x \text{N}^+/\text{P}^+$ junction

If we consider the band diagram of the junction at the thermodynamical equilibrium ($V=0$) represented in figure 2, two cases have to be considered.

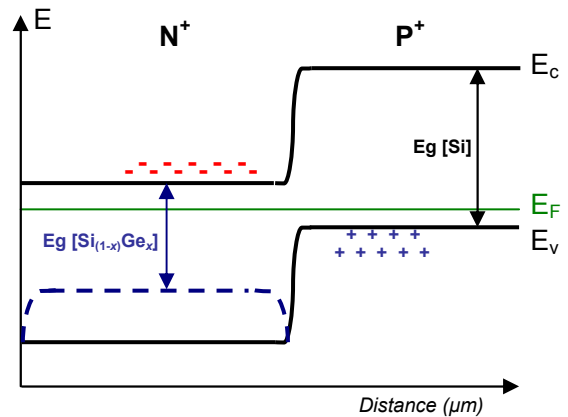


Fig.2 – Schematic of the bands diagram of the P^+/N^+ at the thermodynamical equilibrium

The first one is the case of no germanium in the N^+ layer ($x=0$), the energy gap is the same in the N^+ and in the P^+ parts and is equal to 1.12eV which is the energy gap of silicon at 298K. In the second case, the abrupt germanium profile in the N^+ region induces a reduction of the energy gap which depends on x as illustrated by equation (1) at a temperature equal to 298K and for $x<0.85$ [8].

$$E_g [Si_{(1-x)}Ge_x] = 1.12 - 0.41x \quad (1)$$

At the thermodynamical equilibrium, no current is flowing through the P^+N^+ junction.

If a positive voltage V is applied across the P^+/N^+ junction, then, the junction is forward biased. This corresponds to the P^+ substrate / N^+ buffer configuration of the Trench IGBT when the anode cathode voltage is applied. The band diagram in figure 3 shows a reduction of the voltage barrier due to the difference between the N^+ Fermi level (E_{FN}^+) and P^+ Fermi level (E_{FP}^+), this difference is equal to qV .

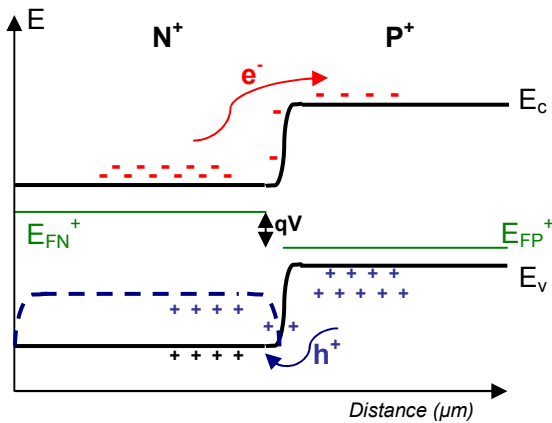


Fig.3 - Schematic of the bands diagram of the forward biased P^+/N^+ junction.

Thus, a diffusion current is created and is flowing through the junction. The electrons diffuse from N^+ region to the P^+ region, and the voltage barriers does not depend on x . It means that the electron injection from N^+ to P^+ does not change with the value of mole fraction x of germanium in the N^+ region. The holes spread from the P^+ to the N^+ region. Meanwhile, the barrier voltage which has to be crossed by the holes decreases with the elevation of x . It means that the hole injection from P^+ to N^+ increases with the value of mole fraction x of germanium in the N^+ region. Furthermore, the interest of using the $Si_{(1-x)}Ge_x$ buffer layer by reducing the energy gap in the N^+ side is to rise the generation recombination rate. This property will be exploited in the case of the proposed IGBT, particularly to reduce the current tail during the turn-off switching.

III. PROPOSED DEVICE STRUCTURE

The proposed device structure is based on a

conventional punch through IGBT controlled by a trench gate. The PNP cathode and the base are separated by a heavily doped N^+ layer (figure 4).

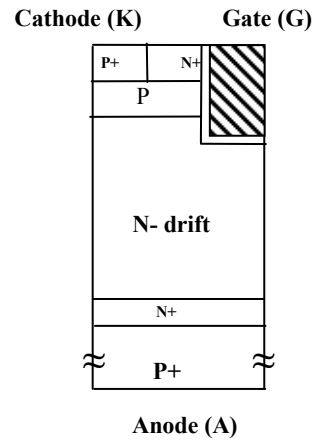


Fig.4 - Conventional Punch Through Trench Gate IGBT

The conventional device model implemented in the finite elements simulator TCAD-SENTAURUS (see section IV for details) has been fitted with experiments for two temperatures and for static and dynamic switching as shown in figures 5 and 6.

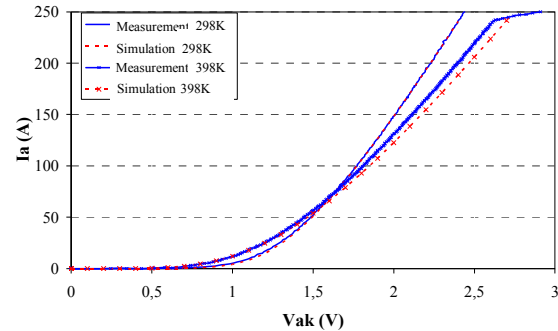


Fig.5 - Simulation and experiment comparison for static characteristic $I_A=f(V_{AK})$ at 298K and 398K of the conventional IGBT

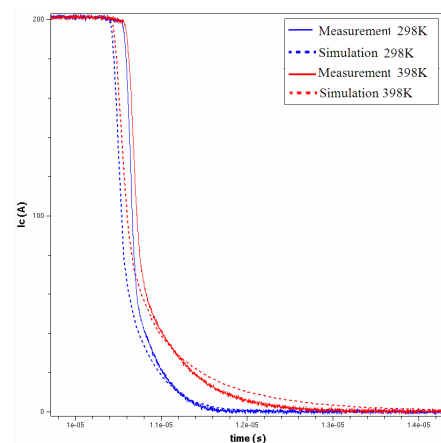


Fig.6 - Simulation and experiment comparison for resistive load switching characteristic at 298K and 398K of the conventional IGBT

Based on this structure, a novel IGBT structure has been designed as shown in figure 7.

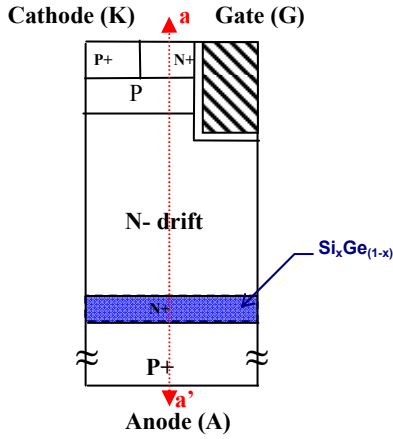


Fig.7 - Novel Punch Through Trench Gate IGBT including $\text{Si}_{(1-x)}\text{Ge}_{(x)}$ N^+ buffer layer

The originality of the proposed device is located in the use of a $\text{Si}_{(1-x)}\text{Ge}_{(x)}$ N^+ buffer layer with an abrupt profile of germanium ($x > 0$). Carriers lifetime is controlled by ion implantation and is uniform in all the structure. In addition to the global carrier lifetime, a local control carrier lifetime has been applied around the $\text{Si}_{(1-x)}\text{Ge}_{(x)}$ N^+ buffer layer.

This device is calibrated for a rated current of about 200A and an avalanche breakdown of about 1200V.

IV. FINITE ELEMENTS DEVICE MODEL

The 2D device structure, represented by a half-cell, has been implemented in the finite element physically-based TCAD-SENTAURUS simulation tool. The simulator solves the main semiconductor equations [7] at each node of the 2D mesh representation of the device:

$$\nabla(\epsilon_{\text{Si}} \vec{E}) = -q(p - n + N_D^+ - N_A^-) \quad (2)$$

$$\frac{\partial n}{\partial t} = \frac{1}{q} \nabla \vec{J}_n - U_n \quad (3)$$

$$\frac{\partial p}{\partial t} = -\frac{1}{q} \nabla \vec{J}_p - U_p \quad (4)$$

$$\vec{J}_n = q\mu_n \vec{E}_n + qD_n \nabla n = -q\mu_n \nabla \phi_n \quad (5)$$

$$\vec{J}_p = q\mu_p \vec{E}_p + qD_p \nabla p = -q\mu_p \nabla \phi_p \quad (6)$$

All of these symbols can be found easily in the literature [7]. The simulator uses coupled thermal and electrical solutions to solve for heat flow in semiconductor devices and incorporates local mobility and generation-recombination effects based on lattice temperature given user-defined boundary conditions needed to solve the lattice heating equation:

$$C_h \frac{\partial T}{\partial t} = \text{div}(\kappa \nabla T) + H \quad (7)$$

where C_h is the heat capacitance per unit of volume, κ is the thermal conductivity, T is the local lattice temperature, H is heat generation with primary contribution from Joule heating.

The half-cell is a $2.2\mu\text{m}$ width and $370\mu\text{m}$ depth structure. The description of the mesh is described in figures 8(a) and (b). A very fine mesh has been used in the channel area (top) whereas the mesh is less fine in the $\text{Si}_{(1-x)}\text{Ge}_{(x)}$ N^+ buffer layer and very coarse in the N^- drift region and in the P^+ anode region.

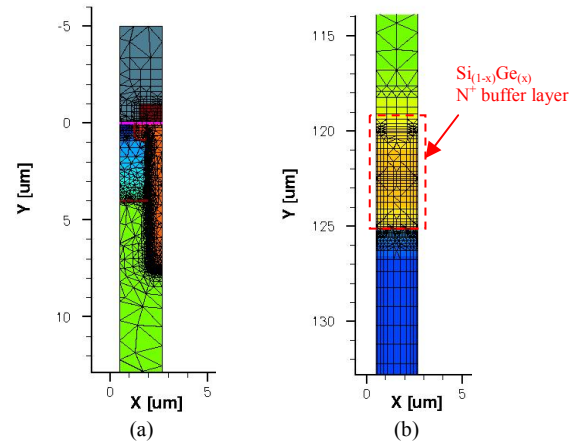


Fig.8 – Description of the mesh : (a) top of the device and (b) $\text{Si}_{(1-x)}\text{Ge}_{(x)}$ N^+ buffer layer

1D analysis can be performed by using the aa' outline as depicted in figure 7. The Shockley Read Hall recombination model can be expressed as follows:

$$R = \frac{np - n_i^2}{\tau_p(n + n_1) + \tau_n(p + p_1)} \quad (8)$$

$$\text{with : } n_1 = n_i \exp\left(\frac{E_{\text{trap}}}{kT}\right); p_1 = n_i \exp\left(\frac{-E_{\text{trap}}}{kT}\right)$$

where E_{trap} is the discrete trap energy related to the intrinsic energy level of the semiconductor, k is the Boltzmann's constant, n_i is the intrinsic concentration and T represents the temperature. The minority lifetimes τ_n and τ_p are modelled as a product of a doping-dependent.

V. SWITCHING PERFORMANCES

One of the main characteristics of the power devices is the maximum switching frequency, directly related to

the switching time. In the case of the IGBT, the turn-off time is related to the capability of the component to sweep away the storage charges (minority carriers) from the N⁻ drift region.

Figure 9 depicts the test circuit used for the simulation of turn-off resistive load at 298K with the evolution of the mole fraction x of germanium in the Si_(1-x)Ge_(x) N⁺ buffer layer from 0% to 40%.

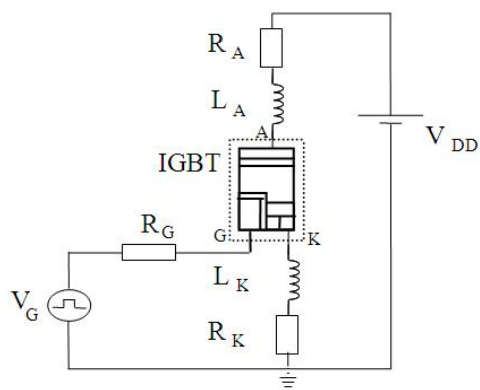


Fig.9 – Simulation of the resistive load turn off at 298K for various mole fraction values

Figure 10 shows that there is a decrease of the turn-off time with the elevation of the mole fraction x of germanium. In fact, the reduction of the energy gap due to the elevation of the mole fraction of germanium in the Si_(1-x)Ge_(x) N⁺ buffer layer, induces a rise of the Shockley Read Hall (SRH) recombination rate in this region.

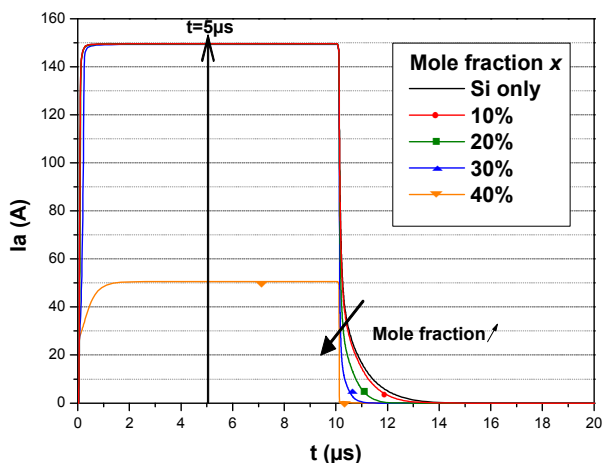


Fig.10 – Simulation of the resistive load turn off at 298K for various mole fraction values

Figure 11 represents the recombination rate taken during the on-state ($t=5\mu s$), with the evolution of the mole fraction x . An elevation of x induces a rise of the recombination rate in the N⁺ buffer layer and thus, a decrease in the N⁻ drift and the P⁺ regions.

Equation (8) confirms that a reduction of the carriers lifetime due to the elevation of x induces a rise of the recombination rate.

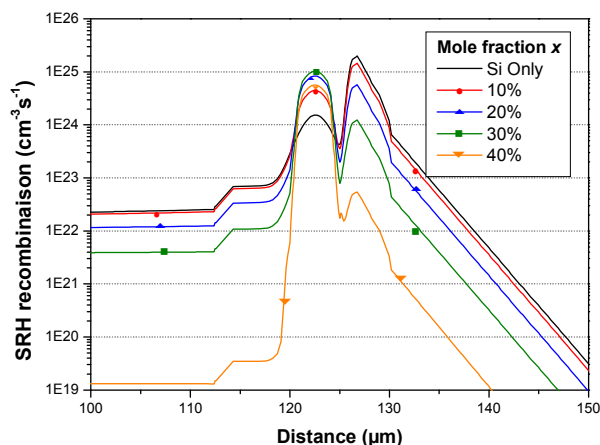


Fig.11 – Simulation of the SRH recombination rate during the resistive load on-state for various mole fractions x along the vertical cut-line a-a'.

During the turn-off, the recombination efficiency of the minority carriers in the N⁺ buffer layer is enhanced with the elevation of the mole fraction x , thus, the current tail is shortened. However, the high carriers recombination rate for a mole fraction exceeding 30% induces an abnormal current waveforms as depicted in figure 10. The recombination rate is so high that it limits the total current during the on-state to a maximum value lower than the normal on-state current value.

Figure 12 represents the anode current versus the anode-cathode voltage for various values of the mole fraction x of germanium in the Si_(1-x)Ge_(x) N⁺ buffer layer. We can observe that the on-state voltage (V_{on}) increases lightly with the elevation of the mole fraction to 20%. Beyond this value, there is a drastic increase of V_{on} .

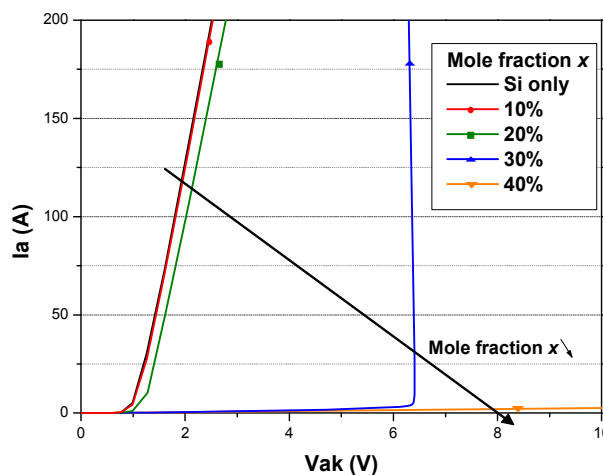


Fig.12 – Simulation of the static characteristic $I_A=f(V_{AK})$ at 298K for various mole fraction values

By considering the IGBT model during the on-state as an association in series of a MOSFET and a PiN rectifier [8], it is possible to express the forward on-state voltage drop V_{on} as a sum-up of the voltage drop across those two components:

$$V_{on} = \frac{2kT}{q} \ln \left[\frac{I_A d}{2kWZD_a n_i F \left(\frac{d}{L_a} \right)} \right] + \frac{I_A L_{CH}}{\mu_{ns} C_{ox} Z (V_G - V_{th})} \quad (9)$$

where W is the width of the N^- drift region, $d = 0.5W$, Z and L_{CH} are respectively the channel width and length, D_a is the ambipolar diffusion coefficient, L_a is the ambipolar diffusion length. $F(d/L_a)$ is an increasing function for d lower than L_a and decreasing for d higher than L_a . μ_{ns} the surface mobility of electrons, C_{ox} the oxide capacitance and V_{th} is the threshold voltage.

In case of an elevation of the mole fraction x in the $Si_{(1-x)}Ge_x N^+$ buffer layer, there is a reduction of carriers lifetime, and thus, the ambipolar diffusion length $L_a = \sqrt{D_a \tau}$ is reduced. By considering the carriers density distribution along the vertical cut-line a-a' and during the on-state, it can be shown that the ambipolar diffusion length L_a is lower than the half width of the N^- drift region d , the function $F(d/L_a)$ decreases inducing the rise of the forward on-state voltage drop V_{on} as expressed in equation (9).

VI. TEMPERATURE DEPENDENCY

Figure 13 presents the turn-off time versus the on-state voltage drop for various values of the mole fraction x of germanium in the $Si_{(1-x)}Ge_x N^+$ buffer layer at various temperatures.

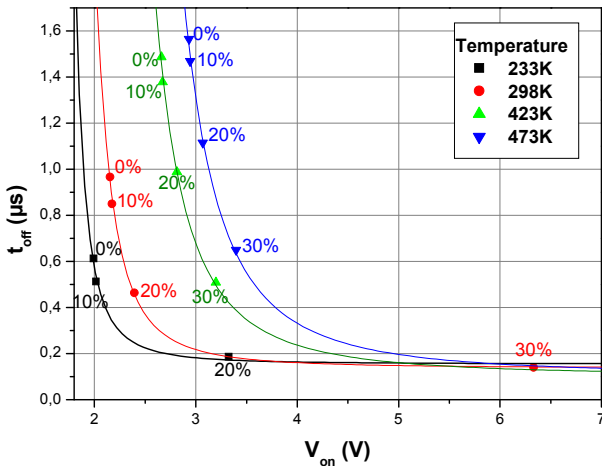


Fig.13 – Trade-off between the turn-off time and the on-state voltage for various mole fraction values and temperature

There is a trade-off between those two parameters with the evolution of x . In fact, at the ambient temperature (298K), for a variation of the mole fraction from 0 to 20%, there is a significant reduction of the turn-off time for a slight elevation of the on-state voltage. Beyond 20% of mole fraction, the rise of the on-state voltage is drastically high. An elevation of the temperature to 423K induces a global elevation of the on-state voltage drop and of the turn-off time for a mole fraction between 0 to 20%. Whereas for $x=30\%$, comparing to the results obtained for a temperature equal

to 298K, there is a slight elevation of the turn-off time but very significant reduction of the on-state voltage. An elevation of the temperature to 473K also induces a global elevation of the on-state voltage and of the turn-off time for various mole fractions comparing to the results obtained for temperatures equal to 298K and 423K. Concerning the low temperature ($T=233K$), for x lower than 15%, there is a global reduction of the on-state voltage and the turn-off time comparing to 298K. A drastic elevation of the on-state voltage happens for x higher than 15%.

The benefit to use $Si_{(1-x)}Ge_x N^+$ buffer layer consists on a significant reduction of the turn-off time for a slight elevation of the on-state voltage. However, the mole fraction x has to be restricted below 20% when considering the temperature dependency, particularly the low temperature effect. In addition to the effect of the mole fraction on the reduction of the turn-off time and the rise of the on-state voltage explained earlier, an elevation of the temperature induces a rise of the on-state voltage, as illustrated in figure 13.

From the previous simulation results, a model of the mole fraction effects on the trade-off between the turn-off time and the on-state voltage has been developed and is represented in figure 13. This model is based on a Lorentzian peak function (10), and is valid for an on-state voltage higher than x_c .

$$t_{off} = y_0 + \frac{2A}{\pi} \left[\frac{w}{4(V_{on} - x_c)^2 + w^2} \right] \quad (10)$$

The parameters used in (9) are presented in table I, where x_c is the center, A is the area, y_0 the offset and w is a parameter called the half width with t_{off} in microseconds and V_{on} in volts. This model allows to predict the trade-off between the on-state voltage and the turn-off time, but its use is restricted to the physical model of the IGBT investigated in this study.

TABLE I

SUM UP OF THE PARAMETERS USED IN THE LORENTZIAN PEAK FUNCTION

Temperature	Area A (10^{-6})	Center x_c	Width w	Offset y_0 (10^{-7})
233 K	1.4864	1.6769	0.20364	1.5415
298 K	1.9802	1.8270	0.35931	1.3636
423 K	6.0004	2.1200	0.50444	1.0247
473 K	6.3411	2.3437	0.63221	1.0666

VII. BLOCKING CAPABILITY

We can observe in figure 14 that an elevation of the mole fraction x of germanium in the $Si_{(1-x)}Ge_x N^+$ buffer layer from 0 to 10%, induces a slight reduction of the static breakdown voltage of the component. For a rise of the mole fraction from 10% to 30%, the breakdown voltages increases and reaches 1300V.

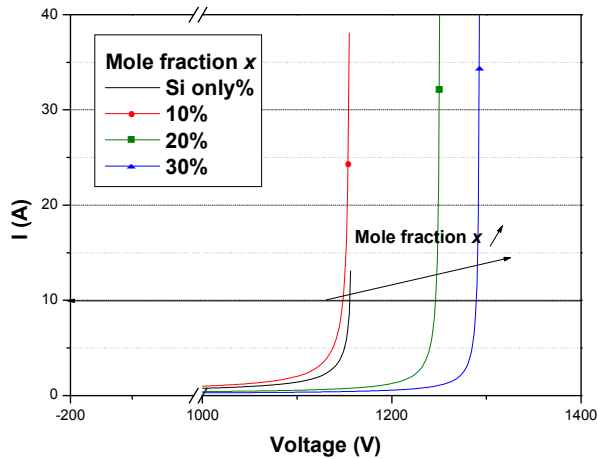


Fig.14 – Simulation of the breakdown voltage for various mole fraction values.

When the breakdown voltage is applied on the device, the avalanche breakdown phenomenon occurs. The elevation of the mole fraction in the N^+ buffer layer from 0 to 30% induces an elevation of the electron-hole recombination rate as shown in figure 15. Then, a reduction of the carriers lifetime slows down the ionization process, by rising the electron-hole recombination efficiency. As a consequence, the breakdown phenomenon happens for a higher breakdown voltage.

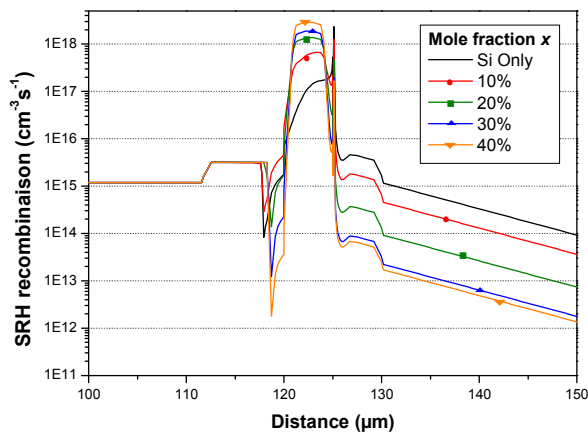


Fig.15 – Simulation of the SRH recombination rate for a current equal to $10\mu A$ and for various mole fractions x under breakdown voltage along the vertical cut-line a-a'.

VIII. EFFECT OF $Si_{(1-x)}Ge_x N^+$ BUFFER LAYER ON SOME OTHER IGBT STRUCTURES : TRADE-OFF COMPARISON

A. Trench Field Stop IGBT [9]

The aim of this device is to propose a vertical shrink of the NPT IGBT to a structure with a thin n- base and a low doped field stop layer to drastically reduce overall losses. Especially the combination of the field stop concept with a trench transistor cell results in the almost ideal carrier concentration for a device with minimum on state voltage and lowest switching losses.

In our study, the $Si_{(1-x)}Ge_x N^+$ buffer has also been added to a Field Stop IGBT (FS-IGBT) and the trade-off

between the turn-off time and the on-state voltage for various mole fraction for a mole fraction varying between 0 to 30% are presented in figure 16. The rise of the mole fraction brings a reduction of the turn-off time. However, this induces an increase of the on state voltage drop, which is drastically high for a mole fraction close to 30%

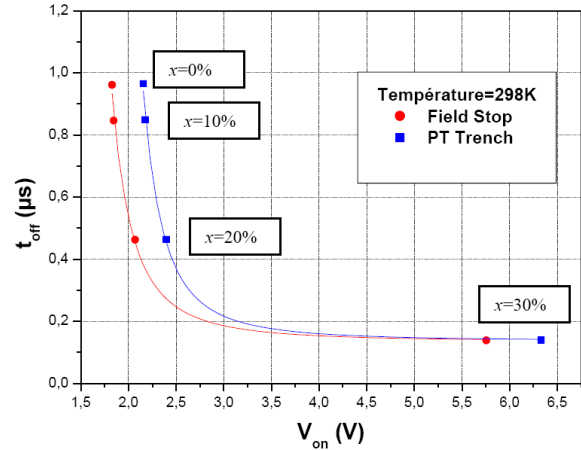


Fig.16 – Trade-off between the turn-off time and the on-state voltage for various mole fractions in the case of a Field Stop structure compared to the PT Trench IGBT

B. Carrier Storage Trench-gate Bipolar Transistor [10]

The main characteristic of this device compared to the conventional PT-IGBT is the use of an additional N^+ layer between the Pbase and the N^- drift region. This structure brings an accumulation of minority carriers in the N^- drift region during the on state leading to an increase of the conductivity in this region, and then to a reduction of the on state voltage drop.

Figure 17 illustrates the effect of the $Si_{(1-x)}Ge_x N^+$ buffer layer for a mole fraction varying between 0 to 30% on a Carrier Storage Trench-gate Bipolar Transistor (CSTBT). It can be highlighted that the effect of the $Si_{(1-x)}Ge_x N^+$ buffer layer is similar for the both devices, except that the CSTBT presents a lower on state voltage drop as well as a higher turn-off time mainly due to its internal structure.

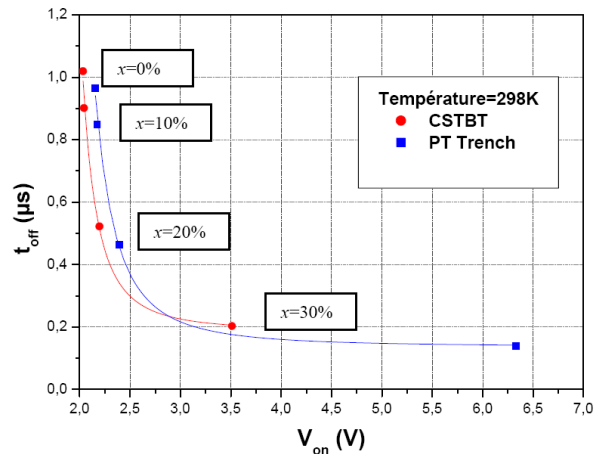


Fig.17 – Trade-off between the turn-off time and the on-state voltage for various mole fractions in the case of a CSTBT structure compared to the PT-Trench IGBT

It is interesting to note that as concerning the turn-off time even if the difference between both devices is constant whatever the mole fraction, the tendency is not the same as regarding the on-state voltage drop variation. Indeed, higher the mole fraction of germanium bigger the difference between both on state voltage drops. This is mainly due to the fact that there is a bigger storage charge in the CSTBT leading to a lower on state voltage drop.

IX. CONCLUSION

A novel Punch Through Trench IGBT using $\text{Si}_{(1-x)}\text{Ge}_{(x)} \text{N}^+$ buffer layer has been investigated with the help of numerical simulations and compared to the conventional PT Trench IGBT. It was highlighted that using $\text{Si}_{(1-x)}\text{Ge}_{(x)} \text{N}^+$ buffer layer with a mole fraction x between 10% and 20% reduces significantly the turn-off time for a slight elevation of the on-state voltage. Furthermore, the effect of the temperature variation on this trade-off has been studied and the results confirm that the mole fraction does not have to exceed 20% to avoid an undesirable rise of the on-state voltage at low temperatures. By taking into account these several results, this new component seems to be a good way to enhance turn-off time for a slight elevation of the on-state voltage by using a mole fraction between 10% and 20% depending on the application needs.

The $\text{Si}_{(1-x)}\text{Ge}_{(x)} \text{N}^+$ buffer has also been added to two types of IGBT showing the improvements mainly made as concerning the on state voltage drop compared to the conventional IGBT structure.

At least, before considering the process itself for the design of this IGBT, the dynamic characteristics and the robustness of the novel IGBT have to be evaluated and compared to the conventional Punch-Through Trench IGBT in terms of short-circuit, clamped and unclamped inductive switching capability.

ACKNOWLEDGMENT

The authors would like to thank Dr. Adel Benmansour and Dr. Jean-Christophe Martin for their participation to this study as former members of the IMS Laboratory.

REFERENCES

- [1] N. D. Jankovic, A. O'Neill "2D device-level simulation study of strained-Si npn heterojunction bipolar transistors on virtual substrates", *Solid-State Electronics*, Volume 48, Issue 2, February 2004, pp 225-230.
- [2] Gang Zhang, John D. Cressler, Guofu Niu, Angelo Pinto "A comparison of npn and pnp profile design tradeoffs for complementary SiGe HBT Technology" *Solid-State Electronics*, Volume 44, Issue 11, 1 November 2000, pp 1949-1954.
- [3] US Patent 6198115 – "IGBT with reduced forward voltage drop and reduced switching loss"
- [4] Tsugutomo Kudoh, Tanemasa Asano "Si/SiGe heterojunction collector for low loss operation of Trench IGBT *Applied Surface Science*", Volume 224, Issues 1-4, 15 March 2004, pp 399-404.
- [5] Fei Zhang, Lina Shi, Chengfang Li, Liang Zhang, Wei Wang, Wen Yu, Xiaowei Sun "Adjustable high-speed insulated gate bipolar transistor" *IEEE Transactions on Plasma Science*, June 2006 Volume: 34, Issue: 3, Part 3, pp: 1021- 1025
- [7] SENTAURUS ISE-TCAD Software, V10
- [8] M E. Levinshtein, S L. Rumyantsev, M S. Shur : "Properties of advanced Semiconductor Materials", Edn A Wiley Interscience Publication, John Wiley & Sons, Inc.
- [9] T. Laska, M. Münzer, F. Pfirsch, C. Schäffer, T. Schmidt, "The Field Stop IGBT (FS IGBT) – A New Power Device Concept with a Great Improvement Potential", *Proceedings of the 12th ISPSD*, pp.355-358, 2000.
- [10] H. Takahashi, H. Haruguchi, H. Hagino, T.Yamada, "Carrier stored Trench-gate Bipolar Transistor - Bipolar Transistor – A Novel Power Device for High voltage application" *Proceedings of ISPSD 96*, pp349-pp352, 1996